A&A 410, 623–637 (2003)
DOI: 10.1051/0004-6361:20031211

Astronomy & Astrophysics

Testing the "strong" PAHs hypothesis

I. Profile invariance of electronic transitions of interstellar PAH cations

G. Malloci[1,2], G. Mulas[1,⋆], and P. Benvenuti[2,3,⋆⋆]

[1] INAF - Osservatorio Astronomico di Cagliari - AstroChemistry Group, Strada n. 54, Loc. Poggio dei Pini, 09012 Capoterra (CA), Italy
[2] Dipartimento di Fisica, Università degli Studi di Cagliari, S.P. Monserrato-Sestu Km 0.7, 09042 Cagliari, Italy
[3] Space Telescope-European Coordinating Facility, ESA, Karl-Schwarzschild-Strasse 2, 85748 Garching bei Munchen, Germany

Received 15 April 2003 / Accepted 5 August 2003

Abstract. The so-called "strong" Polycyclic Aromatic Hydrocarbons (PAHs) hypothesis postulates that isolated PAHs, which are thought to be the carriers of the Unidentified Infrared Bands, ought to be also responsible for a large number of Diffuse Interstellar Bands (DIBs). In this framework, the spectral profile of such DIBs should be due to unresolved rotational structure of vibronic absorption bands, the rotation of the molecule being by and large governed by the interaction with the interstellar radiation field. In this paper we quantitatively test the above hypothesis against the observational constraint of DIBs profile invariance, by using Monte-Carlo methods to model the photophysics of a prototypical interstellar PAH, namely the ovalene cation ($C_{32}H_{14}^{+}$). Our results show that the predicted rotational band profiles are remarkably insensitive to both the ambient conditions and the assumed values of some poorly known parameters. The present model therefore offers a quantitative link between any given PAH and the observed DIB profiles, providing a valuable tool for molecular identification.

Key words. astrochemistry – line: identification – line: profiles – molecular processes – ISM: lines and bands – ISM: molecules

1. Introduction

The Diffuse Interstellar Bands (DIBs), one of the longest standing open problems of astronomy, are absorption features observed in the near-UV, Vis and near-IR spectra of stars reddened by interstellar dust (see e.g. the review by Herbig 1995). Since their first detection about 80 years ago, ~300 DIBs have been discovered in about one hundred sightlines in the Galaxy, and their number keeps growing along with instrument sensitivity (Jenniskens & Desert 1994; Tuairisg et al. 2000; Weselak et al. 2000; Galazutdinov et al. 2000). DIBs were also detected in extragalactic objects, e.g. in Magellanic Clouds (Ehrenfreund et al. 2002).

Over the years, many hypotheses have been formulated about their origin, ranging from impurities embedded in dust grains to gas-phase free molecules (Herbig 1995). Currently, gas-phase carbon based molecules, such as polycyclic aromatic hydrocarbons (PAHs), fullerenes and linear carbon chains, which are thought to be ubiquitous throughout interstellar space, have been proposed as plausible candidate DIB carriers (Ehrenfreund & Charnley 2000). In particular PAH molecules were proposed as attractive DIB carrier candidates due to their photostability (Crawford et al. 1985; van der Zwet & Allamandola 1985; Léger & D'Hendecourt 1985), which is brought about by the delocalization of π electrons over their carbon skeleton. In the so-called "strong" PAH hypothesis these molecules are actually thought to be ubiquitously abundant in the ISM, and to be responsible of the so called Unidentified Infrared Bands (UIBs) in the near and middle infrared (Allamandola et al. 1989), of the far-UV rise of the interstellar extinction curve (Joblin et al. 1992) and of the DIBs (Salama et al. 1999); quite generally, they are believed to be a key element for the chemistry and global energy balance of the interstellar medium (for a recent review, see e.g. Salama 1999 and references therein). The detection of the basic aromatic unit benzene by Cernicharo et al. (2001), one of the many success of the *Infrared Space Observatory*, shows that the physical conditions prevailing in specific interstellar environments are able to activate a rich and diverse chemistry (Woods et al. 2002).

One important implication of the "strong" PAH hypothesis that is seldom mentioned in the literature is that the failure to identify PAH absorption bands in the visible (i.e. among DIBs) would cast strong doubts on the suitability of the PAHs model,

Send offprint requests to: G. Malloci,
e-mail: gmalloci@ca.astro.it
⋆ e-mail: gmulas@ca.astro.it
⋆⋆ e-mail: pbenvenu@eso.org

at least in its broadest interpretation. In short, it should be properly emphasized that the hypotheses for PAHs being responsible respectively for UIBs and DIBs either stand together or fail together.

The identification of large carbon-bearing molecules such as PAHs could yield important improvements in our knowledge of the physics and chemistry of the ISM, which in turn would also have a large impact on our understanding of the formation and evolution of prebiotic organic molecules (see e.g. Bernstein et al. 1999). More directly, since the abundances of dust forming elements such as carbon required by any dust model seem to be larger than those available in the ISM, any firm identification of large, organic molecules would place strong constraints on the well-known problem of the "carbon-crisis" (Cardelli et al. 1996). In spite of the considerable laboratory and observational work based on direct comparisons of the spectral positions (see e.g. Salama et al. 1999; Motylewski et al. 2000; Ruiterkamp et al. 2002) and some promising candidates (Foing & Ehrenfreund 1994; Tulej et al. 1998; Salama et al. 1999), no such firm identification has been established yet.

Spectral positions and intensity ratios, however, are not the only observable DIB property which we can use for their identification. Their spectral profiles are known to be extremely stable across widely different sightlines, and very high resolution observations detected fine structure which is strikingly similar to partially resolved rotational structure of vibronic bands in gas-phase polyatomic molecules (Sarre et al. 1995; Ehrenfreund & Foing 1996; Jenniskens et al. 1996; Kerr et al. 1996; Krelowski & Schmidt 1997; Kerr et al. 1998; Walker et al. 2001; Galazutdinov et al. 2002). A study of rotational profiles of gas-phase molecular absorption bands in interstellar conditions is thus important to test potential DIBs carriers effectively. Several researchers theoretically modelled DIB profiles as rotational profiles in thermodynamical equilibrium (see e.g. Cossart-Magos & Leach 1990). However, Rouan et al. (1992) demonstrated that the population of rotational levels of an isolated, large molecule in interstellar conditions is *qualitatively* different from a thermodynamic equilibrium population. Mulas (1998) later *quantitatively* modelled the detailed photophysics of a generic "interstellar PAH", as described e.g. by Léger et al. (1989), simulating its absorption of UV/Vis photons and the following infrared emission cascades, using Monte-Carlo techniques to keep track of molecular rotation.

In this work we used the above model on a specific PAH, in order to quantitatively test the derived rotational profiles of its vibronic bands against the observed invariance of DIB profiles. More precisely, as a good middle-sized representative of the class, we modelled the ovalene cation $C_{32}H_{14}^{+}$ and its first permitted electronic transition $D_0 \rightarrow D_2$, which happens to fall in the near infrared at about 9700 Å (Ehrenfreund et al. 1992, 1995). We do not mean to claim that the ovalene cation is the best DIB candidate at hand among PAHs, since recent results (Ruiterkamp et al. 2002) actually seem to cast doubts about its presence in the diffuse ISM; we just chose a molecule representative of this class, suitable as a test case, so that many of the results which we obtain can be expected to show general properties of PAHs. Furthermore, the present model can be trivially tailored to any other large molecule under relatively weak assumptions (Mulas 1998), so that the present implementation should also be regarded as a "proof of concept" for its validity as a diagnostic tool. We do plan to apply this same approach to a wide range of molecules in this class, including e.g. larger molecules, different hydrogenation and ionisation states, possibly nitrogen substituted species. In particular, anions and multiply charged cations, whose presence in many interstellar environments has been predicted (see e.g. Bakes et al. 2001a,b, and references therein) are expected to show electronic absorption bands in the visible wavelength range. However this is outside of the scope of the present paper, as stated above, and will be the subject of forthcoming works.

In Sect. 2 we will outline the general assumptions of our theoretical approach. In Sect. 3 we describe how we obtained the input parameters needed to our Monte-Carlo model, i.e. the different ambient interstellar conditions assumed and the molecular parameters. In Sect. 4 we report the resulting predicted "DIB" spectral profiles and we then discuss in Sect. 5 the relations (or lack thereof) between the different possible assumptions and the obtained results. Moreover, since some authors (Webster 1996; Walker et al. 2000) recently proposed isotopic substitutions as a possible explanation of some of the observed fine structure within the profile of some DIBs, most notably the one at 6614 Å, we quantitatively studied the impact of the most likely isotopic substitutions ($^{13}C \rightarrow ^{12}C$ and $D \rightarrow H$) on the profile of the modelled "DIB" at about 9700 Å. This is a straightforward sideproduct of our approach which uses ab initio calculations to obtain ground-state vibrational and rotational properties of the simulated molecule.

2. Theoretical approach

In a first (good) approximation, the rotational structure of a (electric dipole permitted) electronic absorption band depends on the principal momenta of inertia of the molecule, considered as a rigid rotating body, and on the population of the rotational levels before the transition. The momenta of inertia may be different in the two vibronic levels involved in the transition, this difference being of the order of a few percent for large molecules such as PAHs, in which the geometry distortion of excited states, far from the dissociation limit, is expected to be small (Herzberg 1991a,b).

The rotational levels of a quantum rigid rotating body are known, as well as the selection rules governing transitions among them and their relative intensities in electric dipole approximation (Herzberg 1991b). In the isolation conditions experienced by a molecule in the ISM, the population of rotational levels is not in thermodynamic equilibrium at the kinetic temperature of the gas, but is driven by the interaction with the radiation field through a complex statistical equilibrium (Omont 1986; Rouan et al. 1992; Mulas 1998). For example, the estimates of Omont (1986) give for the rate of events of UV photon absorption a characteristic time of 10^4 s and 5.0×10^6 s for a mean PAH molecule in a typical reflection nebula (RN) and in the diffuse interstellar medium (DISM), respectively. The rate of elastic collisions with the dominant

species in the gas, hydrogen atoms and molecules, is estimated to be of the order of 6.0×10^5 s in a RN and 2.0×10^7 s in the DISM. The interaction with the exciting radiation field, therefore, is likely to completely dominate the population and depopulation of the rotational levels of the ground vibronic state, from which the molecule produces its absorption bands. This state of affairs quickly leads to the establishment of a statistical equilibrium which is not representable as a thermal equilibrium. The strictly stochastic character of this process makes it suitable to be studied using Monte-Carlo techniques. We make use of the approach described by Mulas (1998), and here describe only its extensions in the present work. We refer the reader to the original paper for further details.

In Mulas (1998) the "molecule" under study was considered as a completely closed, isolated system, whose evolution was simulated only through the absorption of UV/Vis photons and the subsequent deexcitation via IR emission cascades. This approach is only correct if the given species stays in this state for a sufficiently long time to reach statistical equilibrium, so that its previous history is completely "forgotten" and becomes irrelevant. By "species" we here mean a given molecule in a given ionisation state. The time it takes to reach such a statistical equilibrium depends obviously on how far from it the starting situation is. To quantitatively estimate this characteristic time, we ran the model on a starting population of rotational states very far from the equilibrium condition and verified how many cascades were necessary for the population to effectively lose all memory of its previous state and then approach and begin oscillating around the equilibrium condition. Figure 1 shows the predicted rotational profiles of the modelled band as a function of the number of infrared cascades, showing that it takes about 60 of them for the population to "forget" its starting point in the specific case considered.

Therefore, a given "molecular state" can be reliably modelled as isolated if and only if its lifetime allows it to forget its previous history. If, on the other hand, a few molecular states (such as different charge and/or hydrogenation states) are interconnected with sufficently high rates, the rotation of the molecule must be followed along its evolution in a random walk among all of these states, which is relatively straightforward using the same Monte-Carlo techniques described in Mulas (1998).

2.1. Interconnected molecular states

Let us consider the main different "molecular states" which may be important for the rotation of the molecule under study. A good discussion concerning the physical and chemical processes related to interstellar PAHs can be found in Vuong & Foing (2000); Le Page et al. (2001). The competing processes involving the hydrogenation and charge states of a generic PAH in diffuse interstellar clouds are given, respectively, by:

1. photodissociation $\Longleftrightarrow$ chemical reactions,
2. photoionization $\Longleftrightarrow$ electronic recombination.

The probabilities of the main dissociation channels, the loss of atomic and molecular hydrogen, have been estimated by Allain et al. (1996a,b) for several PAHs. The rates they obtained are given in Table 1 for both neutral ovalene and its cation. The processes competing with such photodestructive channels are chemical reactions with the most aboundant element, the hydrogen atom. Vuong & Foing (2000) estimated the addition coefficient of H atoms to be 9.6×10^{-11} cm^3 s^{-1} for $C_{32}H_{14}^+$ and about 10^{-11} cm^3 s^{-1} for $C_{32}H_{14}$ (cf. Table 1).

Therefore, assuming a hydrogen density $n_{\rm H}$ of about 10 cm^{-3} and a mean photon asborption rate for a middle-sized PAH of $\sim 5.0 \times 10^{-8}$ s^{-1}, we obtain that the ovalene molecule will, on the average, go through many tens of UV/Vis photon absorptions and consequent IR cascades before undergoing (de)hydrogenation. We therefore consider

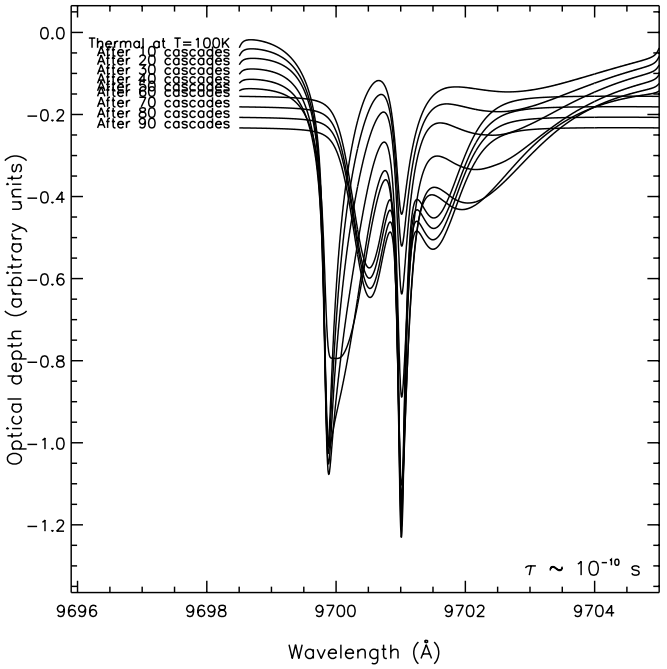

Fig. 1. The evolution of the expected rotational profile of the $D_0 \rightarrow D_2$ electronic transition of $C_{32}H_{14}^+$ for a population of molecules starting in thermal equilibrium ($T \sim 40$ K), after the absorption of a given number of UV/Vis photons and the consequent IR emission cascades. Despite starting far from the statistical equilibrium, after 60 cascades the profile converges to the latter, thereafter just oscillating around it.

Table 1. Rates of the main processes affecting the hydrogenation state of both $C_{32}H_{14}$ and $C_{32}H_{14}^+$. Photodissociation rates are taken from Allain et al. (1996a,b), while reaction rates with H atoms are obtained using the addition coefficients of $\sim 10^{-11}$ cm^3 s^{-1} for the ovalene neutral and 9.6×10^{-11} cm^3 s^{-1} for the cation (Vuong & Foing 2000), assuming $n_{\rm H} = 10$ cm^{-3} (Omont 1986). For comparison, the typical photon absorption rate for a middle-sized PAH is 5.0×10^{-8} s^{-1} (Omont 1986).

Process	$C_{32}H_{14}$	$C_{32}H_{14}^+$
H loss	1.78×10^{-10} s^{-1}	7.33×10^{-10} s^{-1}
H_2 loss	4.85×10^{-11} s^{-1}	2.0×10^{-10} s^{-1}
H addition	$\sim 10^{-10}$ s^{-1}	9.6×10^{-10} s^{-1}

different hydrogenation states to be disjoint and independent as far as rotation is concerned.

Let us now consider the effect of ionisation. The electronic recombination rate $R_{\rm rec}$ is given by $k_{\rm rec}\, n_{\rm e}$, where $k_{\rm rec}$ and $n_{\rm e}$ are the recombination coefficient and the electron density, respectively. Concerning the electron recombination coefficient, Kin-Wing et al. (2001) pointed out that different approximations are adopted by different authors, which result in differences of about 1−2 orders of magnitude in their respective estimates. The ionization fraction of interstellar PAHs is an open question in the literature and laboratory measurements of $R_{\rm rec}$ for a large sample of PAHs are needed. Lacking a consensus on commonly accepted values, we ran our model with a grid of $R_{\rm rec}$ covering the above range, in order to estimate its impact on the final results. We used the following three different approximations:

$$k_{\rm rec}({\rm cm^3\,s^{-1}}) = 1.66\times10^{-5}\sqrt{\frac{100}{T({\rm K})}}\sqrt{\frac{N_{\rm C}}{50}} + 6.3\times10^{-8}\sqrt{\frac{T({\rm K})}{100}}\frac{N_{\rm C}}{50}, \quad (1)$$

$$k_{\rm rec}({\rm cm^3\,s^{-1}}) = 1.0\times10^{-6}\sqrt{\frac{300}{T({\rm K})}}, \quad (2)$$

$$k_{\rm rec}({\rm cm^3\,s^{-1}}) = 3.0\times10^{-7}\sqrt{\frac{300}{T({\rm K})}}. \quad (3)$$

Equation (1) is the well known Spitzer's approximation for small grains, in the form obtained by Vuong & Foing (2000), in which classical electrostatic theory gives an expression proportional to the number of carbon atoms $N_{\rm C}$. The other two expressions stem from the laboratory measured electron recombination rates at 300 K for benzene cation and naphtalene cation respectively (Abouelaziz et al. 1993), previously used e.g. by Salama et al. (1996). Following Omont (1986), if we assume an electron density of 10^{-2} cm^{-3} and a temperature of 100 K for the diffuse interstellar medium, the previous expressions, taking $N_{\rm C} = 32$ in the first one, give for $R_{\rm rec}$ the values of 1.3×10^{-7}, 1.7×10^{-8}, 5.2×10^{-9} s^{-1}, respectively. With the above electronic recombination rates we obtain very different situations concerning the rotation of the molecule under study, including the two opposite extreme cases:

1. If we use the lowest electron recombination rate of the order of 10^{-7} s^{-1}, the molecule will spend relatively long times in its cationic state. It will, in this state, undergo sufficiently many UV/Vis photon absorptions and subsequent IR emission cascades to completely forget its previous history, and therefore this "molecular state" can be considered independently of any others as far as rotation is concerned.
2. If we assume the highest electron recombination of about 10^{-7} s^{-1} rate, the ovalene cation will promptly recombine after its formation, hence its rotation will essentially be the same of its parent neutral molecule. On the other hand, the neutral molecule will remain neutral long enough to relax to its rotational statistical equilibrium as an isolated system. Therefore, the cation will rotate as its parent neutral molecule in its statistical equilibrium. This approximation corresponds to neglecting both the angular momentum change due to ionisation itself (which is of the order or a few $\hbar$ units at most, for the energies involved) and the IR cascade produced by the possible residual excitation energy in excess with respect to the first ionisation potential, retained by the cation, which is acceptable for our purposes.

The above extreme possibilities are the simplest ones to study, since in both cases the Monte-Carlo model only needs to take into account one molecular state at a time. If we, on the other hand, assume an intermediate electron recombination rate of $\sim10^{-8}$ s^{-1}, the molecule changes its ionisation state with rates comparable to the UV/Vis photon absorption rate which govern its rotation. This case is more complicated but still tractable within our scheme, following the evolution of the rotation of the molecule through its subsequent ionisations and recombinations. Every time it changes its charge state, the population of rotational levels is retained from its precursor, i.e. we assume the direct impact of ionisation and/or recombination on rotation to be negligible, being of the same order of magnitude as that of elastic collisions (see e.g. Omont 1986). The absorption of UV/Vis photons and the consequent IR cooling are modelled using the appropriate absorption cross sections, vibrational frequencies and Einstein coefficients for the specific ionisation state of the molecule. In this way, the overall system including a population of interacting neutral and cation ovalene molecules reaches a statistical equilibrium condition which can, in principle, be different from the ones obtained by considering them as disjoint populations.

The model by Mulas (1998) in its original implementation was capable to take in input a population of molecules and evolve it through any given number of UV/Vis photon absorptions and subsequent IR cooling cascades. The enhancement developed for the present work can be outlined as follows:

1. calculate a random number i of non-ionising photons which a neutral ovalene molecule will absorb before the $(i+1)$th one which ionises it;
2. evolve the population of neutral ovalene molecules through the absorption of i photons using the original model;
3. "ionise" the molecule, retaining the same population of rotational levels of the precursor neutral;
4. calculate a random number j of photons which the ovalene cation will absorb before recombination;
5. evolve the population of ovalene cation molecules through the absorption of j photons using the original model;
6. "neutralise" the molecule, retaining the same population of rotational levels of the precursor cation;
7. continue from the first step, and iterate until an overall statistical equilibrium is reached.

We therefore proceed to evaluate the distributions of the number of absorbed photons i and j.

The probability $p_{\rm ion}$ for the neutral molecule to be ionized after the absorption of a photon can be obtained as the ratio

between the ionization rate $R_{\rm ion}$ and the absorption rate of the neutral $R^{\rm N}_{\rm abs}$:

$$p_{\rm ion} = \frac{R_{\rm ion}}{R^{\rm N}_{\rm abs}}. \quad (4)$$

The probability p_i for the molecule being ionized by the absorption of the $(i+1)$th photon is simply given by:

$$p_i = (1 - p_{\rm ion})^i \, p_{\rm ion} = q^i_{\rm ion} \, p_{\rm ion},$$

where $q_{\rm ion}$ is the probability of the opposite event.

Likewise, we define $p_{\rm neu}$ as the probability for the cation to neutralise by electron capture before absorbing a photon. Since electron recombination and photon absorption by the cation are mutually exclusive events, $p_{\rm neu}$ is given by the ratio:

$$p_{\rm neu} = \frac{R_{\rm rec}}{R_{\rm rec} + R^{\rm C}_{\rm abs}}, \quad (5)$$

between the recombination rate for electron and positive ion $R_{\rm rec}$, and the sum between $R_{\rm rec}$ and the absorption rate of the cation $R^{\rm C}_{\rm abs}$. Hence, the probability p_j for the cation molecule to absorbe j photons and then recombine before absorbing the $(j+1)$th is simply given by:

$$p_j = (1 - p_{\rm neu})^j \, p_{\rm neu} = q^j_{\rm neu} \, p_{\rm neu}.$$

Generators of random numbers following many well known distributions are largely available. We made use of GSL (GNU Scientific Library 2001), specifically adopting the function gsl_rng_uniform_pos which returns a positive (double precision) number uniformly distributed in the range (0, 1).

We also estimated the rates connecting the neutral charge state to the anion and the cation with the dication respectively, and they turned out to be very small under any assumptions, so that they never needed to be taken into account to study the rotation of the cation. For example, using the formalism in Allamandola et al. (1989) to estimate the rate of electron attachment to neutral ovalene, we obtain $R_{\rm anion} = S_{\rm e} k_{\rm e} n_{\rm e} \simeq 10^{-8}\ {\rm s}^{-1}$ assuming an electron sticking coefficient $S_{\rm e} \simeq 5\times10^{-2}$ (Allamandola et al. 1989), a rate of collision with electrons $k_{\rm e} \simeq 1.3 \times 10^{-6}\ {\rm cm}^3\,{\rm s}^{-1}$ (Le Page et al. 2001) and an electron density $n_{\rm e} \simeq 1.4\times10^{-1}\ {\rm cm}^{-3}$ (for a reflection nebula as the Red Rectangle, the most favorable case we considered here). Such a low $R_{\rm anion}$ makes negative ionisation a very rare event with respect to photon absorption, with the consequence that the neutral molecule (let alone the cation) will always completely "forget" having been an anion as far as its rotation is concerned.

3. Input parameters

The Monte-Carlo model takes in input:

1. the absorption cross-section $\sigma_{\rm abs}(E)$ of the molecule up to the Lyman limit at 13.6 eV;
2. the spectrum of the exciting radiation field expressed as number of photons $N(E)$ with energy between E and $E + {\rm d}E$ per unit area and unit time;
3. the full vibrational analysis for the ground state within harmonic approximation, specifically the symmetries and oscillator strengths of all IR-active modes;
4. the principal momenta of inertia for both states involved in the transition, i.e. the rotational level structure, and the matrix elements of the rovibrational transitions.

We now separately discuss each item of the above list.

3.1. The absorption cross-sections

A good review on the spectroscopy of PAHs and their ions was given by Salama (1999). Cationic PAH molecules have been the target of much laboratory study in recent years, mainly using matrix isolation spectroscopy. UV/Vis/NIR absorption spectra of the neutral and cation ovalene obtained with this technique are available in the literature (Ehrenfreund et al. 1992, 1995; Ruiterkamp et al. 2002). The spectrum of the neutral molecule is characterised by three principal absorption band systems, falling around 2158 Å, in the 2700−3400 Å range and in the 3400−4300 Å window, respectively. After VUV irradiation of the sample new features arise in the spectrum at 4632, 5357, 5621 and 9750 Å (Ruiterkamp et al. 2002). With respect to the VUV range (from ∼7 eV up to the Lyman limit of 13.6 eV), there is generally very little data available on PAHs. Among them, the high temperature gas-phase absorption spectra of neutral PAHs performed up to ∼17.73 eV by Joblin et al. (1992), show that the absorption cross-section $\sigma_{\rm abs}(E)$ increases smoothly at energies above ∼7.4 eV to a maximum at ∼17.4 eV in a single broad absorption peak composed of $\sigma^* \leftarrow \sigma, \sigma^* \leftarrow \pi, \pi^* \leftarrow \sigma$ and Rydberg spectral transitions (Joblin 1992; Leach 1995).

Although no VUV data are available for PAH ions as far as we know (Salama et al. 1999), the spectrum of the ion is expected to resemble the spectrum of the neutral for the higher excited states, implying rather strong transitions in the VUV, since the $\sigma^* \leftarrow \sigma$ transition should be largely unaffected by ionisation (Joblin 1992; Leach 1995; Salama 2002; Gudipati 2002). Along these lines, Robinson et al. (1997) estimated the electronic absorption cross-section of the cation of ovalene, at energies higher than their experimental limit, at about 7.75 eV, by fitting the spectrum for the neutral molecule in Joblin (1992) with Lorentzians and then subtracting the features thought to be due to $\pi^* \rightarrow \pi$ transitions, which should not contribute significantly to the absorption spectrum of the ion.

In the present work we performed our simulations using both of the alternative spectra for the ovalene cation provided by Robinson et al. (1997), in order to explicitly estimate the impact of this source of uncertainty on our results.

3.2. The exciting radiation fields

We ran independent simulations using four different radiation fields, corresponding to a very wide range of radiation densities and UV flux fraction, in order of decreasing hardness:

1. the radiation field illuminating a specific planetary nebula, IRAS 21282+5050, according to Pech et al. (2002);

2. two different interstellar radiation fields of Mathis et al. (1983), estimated for the galactic plane at different galactocentric distances;
3. the radiation field exciting a specific reflection nebula, the Red Rectangle, as given by Men'shchikov et al. (1998).

All the above radiation fields correspond to typical environments in which UIBs are observed, i.e. in which free flying PAH-like molecules are expected to be abundant.

The total background interstellar radiation field in the range 4.5−13.6 eV has been measured by Gondhalekar et al. (1980) using the observations over the whole sky performed with the ultraviolet sky-survey telescope. However our model also needs the flux of lower energy photons, since they may contribute significantly to the photophysics of the ovalene cation, which displays a strong absorption near 9750 Å (∼1.3 eV); hence, following Dartois & D'Hendecourt (1997), we chose to use the background interstellar galactic fields obtained by Mathis et al. (1983) in the range 900−80 000 Å, using stellar population models. The first box of Fig. 2 shows the five curves corresponding to the galactocentric distances of 5, 6, 8, 10 and 13 kpc, respectively, along with the line connecting the data points measured by Gondhalekar et al. (1980). We remark that the interstellar radiation field theoretically estimated by Mathis et al. (1983) for a galactocentric distance of 10 kpc is in good agreement with the results of Gondhalekar et al. (1980).

Following Pech et al. (2002) we represented the flux from the central star illuminating IRAS 21282+5050 using a Kurucz atmospheric model (see Kurucz 1992); in particular, the models most closely matching the parameters of the star which powers the nebula, of spectral type O7(f)-[WC11], are those with $T_{\rm eff}$ = 28 000 K. The results of the Monte-Carlo model are completely insensitive to the $\log g$ and metallicity chosen. Given a distance of about 3 kpc and a total luminosity of $L = 5.3 \times 10^3\ L_\odot$ for this specific source as found in Pech et al. (2002), the flux of the corresponding Kurucz model has been scaled by the blackbody dilution factor $W_{\rm dil} = 2.44 \times 10^{-11}$ obtained by combining the inverse square law and the Stefan-Boltzmann equations:

$$W_{\rm dil} = \frac{F}{F_{\rm surf}} = \frac{L}{4\pi d_\star^2} \frac{1}{\sigma T_{\rm eff}^4}, \qquad (6)$$

where $\sigma = 5.670 \times 10^{-8}\,{\rm W\,m^{-2}\,K^{-4}}$ is the Stefan-Boltzmann constant, $T_{\rm eff}$ = 28 000 K, and $d_\star$ is the projected distance corresponding to 1″ from the central source, where the maximum intensity of the UIBs (more specifically of the band at ∼3.3 μm) is observed. We used the same approach to represent the radiation field of the specific reflection nebula considered, which we chose to be the well known Red Rectangle; this is illuminated by the central star HD 44179, of spectral type B9-A0III, which lies at a distance of about 330 pc from us (Cohen 1975). We approximated the radiation field of this star with the Kurucz model corresponding to $T_{\rm eff}$ = 8000 K and $\log g$ = 1.0, as found in Men'shchikov et al. (1998). The dilution factor in this case is $W_{\rm dil} = 3.98 \times 10^{-11}$, obtained from Eq. (6) using $L = 3.0 \times 10^3\ L_\odot$, $T_{\rm eff}$ = 8000 K, and $d_\star$ = 0.08 pc the projected distance on the sky of the sightline ∼1″ away from the central source, where the maximum UIB emission is located (Sloan et al. 1993).

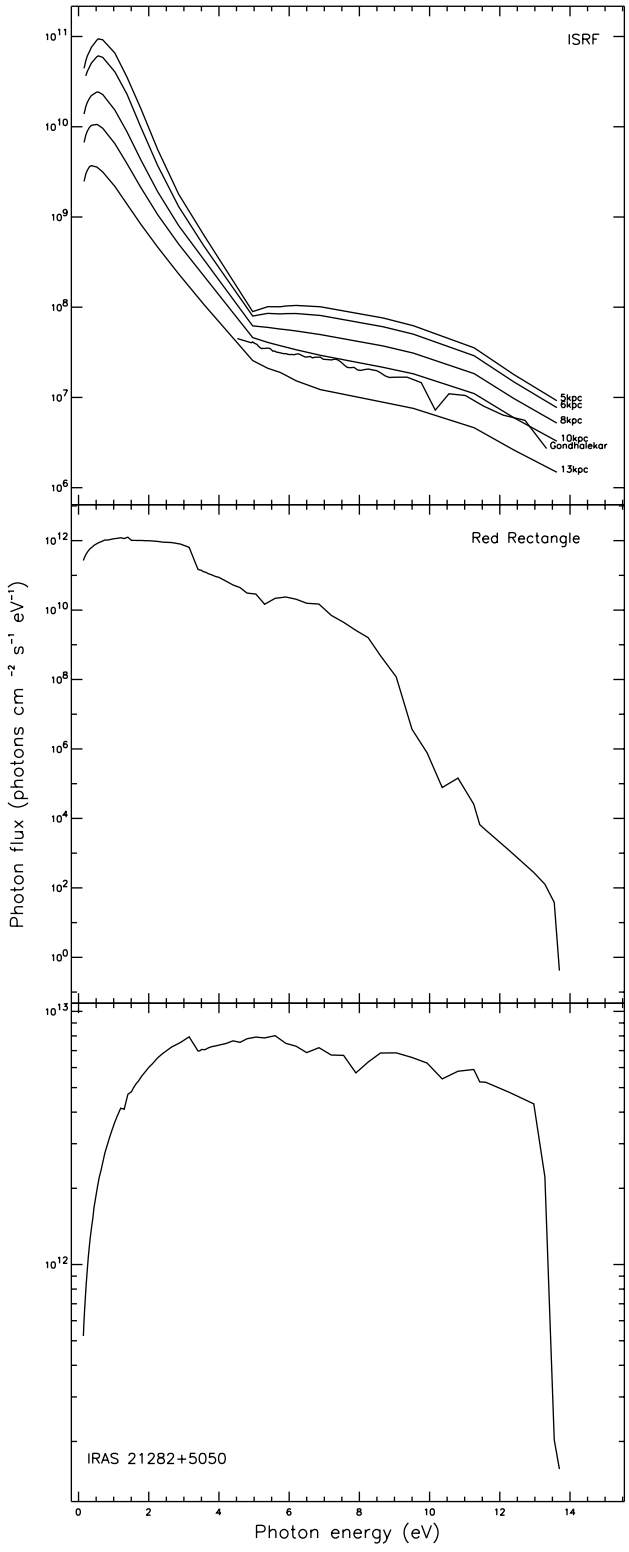

Fig. 2. The top box shows the average interstellar radiation field of Mathis et al. (1983) at different selected galactocentric distances in the range 5−13 kpc along with the UV radiation field observed over the whole sky by Gondhalekar et al. (1980). The middle and bottom boxes display the radiation fields of the stars illuminating the specific reflection and planetary nebulae considered, respectively; both of them were obtained from stellar atmospheric models of Kurucz (1992) scaled by the blackbody dilution factor corresponding to the geometry of the source.

Multiplying the photon number flux $N(E)$ times the absorption cross-section $\sigma_{\rm abs}(E)$ of the molecule yields the rate of photon absorption, according to the equation:

$$R_{\rm abs} = \int_0^{13.6} \sigma_{\rm abs}(E)\, N(E)\, {\rm d}E, \tag{7}$$

where the integral extends over the whole energy range in which the molecule absorbs, up to the Lyman limit at 13.6 eV, since higher energy photons are not present in the radiation fields being considered here. Likewise, the ionization rate can be estimated using the expression

$$R_{\rm ion} = \int_{\rm IP}^{13.6} Y_{\rm ion}(E)\, \sigma_{\rm abs}(E)\, N(E)\, {\rm d}E, \tag{8}$$

where $Y_{\rm ion}(E)$ is the ionization yield and the lower integration limit is the first ionization potential of the molecule. We estimated $Y_{\rm ion}(E)$ for the ovalene molecule according to the expression given by Le Page et al. (2001):

$$Y_{\rm ion}(E) = a\, {\rm e}^{-b[c(E-d)]^4}, \text{ with } \begin{cases} a = 0.8, \\ b = 0.00128, \\ c = 7.6/8.18, \\ d = 14.89\ {\rm eV}, \end{cases}$$

which is the result of a fit to the experimental ionization yelds for pyrene and coronene as measured by Verstraete et al. (1990). Such measurements show that $Y_{\rm ion}(E)$ steeply increases above the IP of the PAH and reaches a limit value of about 0.8 (the constant a) at $\sim$12 $\mu{\rm m}^{-1}$ = 14.89 eV (the term d). The constant c is obtained as the ratio

$$\frac{14.89 - IP_{\rm coronene}}{14.89 - IP_{\rm ovalene}},$$

where the ionization potentials of coronene and ovalene are, respectively, 7.29 eV and 6.71 eV, as found through photoelectron spectroscopy by Eilfeld & Schmidt (1981).

The distribution of the absorption rate as a function of photon energy, defined as ${\rm d}R_{\rm abs}/{\rm d}E = \sigma_{\rm abs}(E)\, N(E)$, is given in Fig. 3 for the neutral and cation ovalene in the different radiation fields considered. In particular, for $C_{32}H_{14}$ we used the absorption cross-section measured by Joblin (1992), while the $\sigma_{\rm abs}(E)$ for $C_{32}H_{14}^{+}$ was obtained by combining the matrix results of Ehrenfreund et al. (1992, 1995) for the UV/Vis/NIR range and both the estimates (cation a and cation b) for the VUV given by Robinson et al. (1997). The resulting total absorption and ionization rates, evaluated according to Eqs. (7)–(8), are presented in Table 2.

The Monte-Carlo model uses the previous information as described in Mulas (1998). It needs to extract in a random way the energy of the asborbed photon; in order to do this, the probability $P(E)$ for the molecule to absorb a photon of a given energy E in a second is evaluated from the knowledge of the radiation field $N(E)$ and the absorption cross-section $\sigma_{\rm abs}(E)$:

$$P(E) = \frac{{\rm d}R_{\rm abs}}{{\rm d}E} = N(E) \cdot \sigma_{\rm abs}(E).$$

The probability distribution thus obtained is integrated to give the cumulative probability distribution and then numerically inverted to obtain the transformation rule relating the uniform

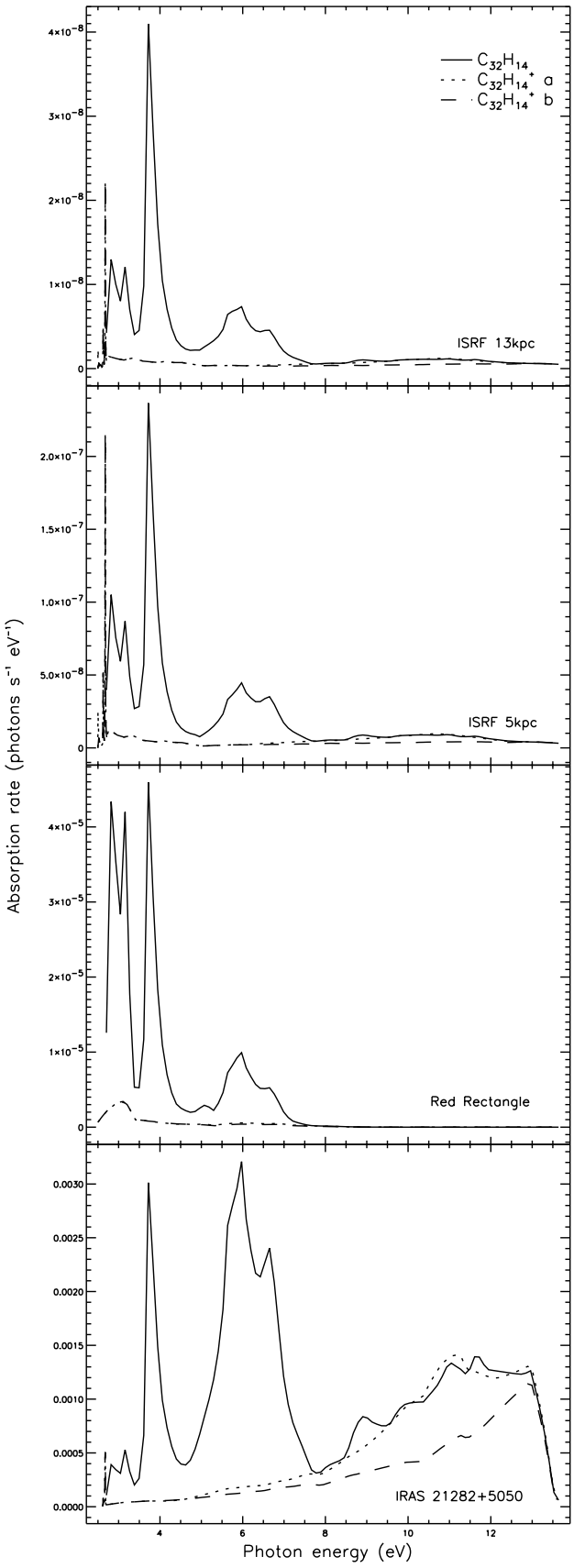

Fig. 3. Distribution of the absorption rate of the ovalene neutral, cation (a) and cation (b), in the different radiation fields considered in units of photons $s^{-1}\,eV^{-1}$.

Table 2. Rates of the main photophysical processes involving $C_{32}H_{14}$ and $C_{32}H_{14}^{+}$ in the different radiation fields considered. The absorption rates are evaluated from Eq. (7) while the ionization rates of the neutral is obtained according to Eq. (8). For comparison, the corresponding electron recombination rates obtained using the electron recombination coefficients expressed by Eqs. (1)–(3) are also given; the electron density is estimated from the carbon atoms density, assuming that all of the available electrons come from the carbon ionization process (we take the cosmic ratio of carbon to hydrogen given by Snow & Witt (1995) equal to $n_e/n_H = 1.4 \times 10^{-4}$). Rates are expressed in units of s^{-1}.

Radiation field	R_{abs}^{N}	$R_{abs}^{C(a)}$	$R_{abs}^{C(b)}$	R_{ion}	R_{rec}^{1}	R_{rec}^{2}	R_{rec}^{3}	T(K)	$n_H(cm^{-3})$	$n_e(cm^{-3})$
PN	1.2×10^{-2}	6.1×10^{-3}	3.8×10^{-3}	3.2×10^{-3}	2.1×10^{-5}	1.7×10^{-6}	5.1×10^{-6}	2.0×10^{4}	1.0×10^{5}	1.4×10^{1}
RR	4.9×10^{-5}	4.3×10^{-6}	4.0×10^{-6}	7.2×10^{-8}	1.9×10^{-6}	2.4×10^{-8}	7.3×10^{-8}	1.0×10^{2}	1.0×10^{3}	1.4×10^{-1}
5 kpc	2.4×10^{-7}	6.5×10^{-8}	4.7×10^{-8}	2.1×10^{-8}	1.9×10^{-7}	2.4×10^{-9}	7.3×10^{-9}	1.0×10^{2}	1.0×10^{2}	1.4×10^{-2}
6 kpc	1.9×10^{-7}	5.1×10^{-8}	3.6×10^{-8}	1.7×10^{-8}	1.9×10^{-7}	2.4×10^{-9}	7.3×10^{-9}	1.0×10^{2}	1.0×10^{2}	1.4×10^{-2}
8 kpc	1.3×10^{-7}	3.2×10^{-8}	2.3×10^{-8}	1.1×10^{-8}	1.9×10^{-7}	2.4×10^{-9}	7.3×10^{-9}	1.0×10^{2}	1.0×10^{2}	1.4×10^{-2}
10 kpc	8.0×10^{-8}	1.9×10^{-8}	1.4×10^{-8}	6.4×10^{-9}	1.9×10^{-7}	2.4×10^{-9}	7.3×10^{-9}	1.0×10^{2}	1.0×10^{2}	1.4×10^{-2}
13 kpc	3.7×10^{-8}	8.5×10^{-9}	6.2×10^{-9}	2.7×10^{-9}	1.9×10^{-7}	$2.4 \times 1o^{-9}$	7.3×10^{-9}	1.0×10^{2}	1.0×10^{2}	1.4×10^{-2}

deviates in the range $(0, 1)$ to the random photon energies distibuted according to the required probability distribution. The results obatined as described above are presented in Fig. 4 for all cases considered.

3.3. Structural and vibrational analysis via ab initio calculations

The knowledge of the structural properties of the molecule of interest enables us to calculate the principal momenta of inertia; the latter are needed to compute the structure of quantum rigid rotor energy levels and the Hönl-London factors (Herzberg 1991b,a) which are used in the simulation. The vibrational analysis is used to compute the probability for spontaneous IR emission in all vibrational bands as a function of the excitation energy. All of the above parameters were obtained through ab initio calculations, which were performed using the NWChem (Northwest Computational Chemistry Package) computer code (Harrison et al. 2001). We used the Density Functional Theory (DFT), which provides a superior ratio of accuracy to computational cost relative to other ab initio methodologies, for the computation of ground state properties of relatively large molecules like PAHs (Langhoff 1996; Hudgins et al. 2001; Bauschlicher Jr. 2002). However, the level of theory implemented in the DFT module of the presently available version of NWChem cannot reliably be used to represent excited electronic states (with some exceptions), nor to compute the corresponding electronic transition moments.

This is currently the major obstacle standing in the way of building a completely self-contained computational machine capable of predicting the expected "DIB" positions and profiles for virtually any interesting molecule, which remains our next, admittedly rather ambitious goal. To achieve this we would need to be able to compute the whole absorption spectrum of any given molecular species up to the Lyman limit. However, a precise knowledge of the positions and intensities of all the transitions up to 13.6 eV is currently out of reach even for state of the art time-dependent DFT codes. The reason is that above about 5 eV Rydberg transitions come into play and although these can be modelled relatively easily, the mixing between them and the valence transitions are very hard to get right, even for very small molecules, let alone for larger ones (Bally 2002).

On the other hand, we want to stress that our model is a statistical approach to the physical processes involved in the UV/Vis photon absorption by the molecule and its subsequent IR cooling; as such, it is very poorly influenced by small errors in the assumed input parameters, provided that they are not systematic. As we will show in more detail in the following sections, our results bring this out very clearly a posteriori.

3.3.1. Ab initio computational details

We obtained the molecular properties of interest using the hybrid exchange-correlation functional B3LYP, as proposed and tested by Becke (1993), in conjunction with the Gaussian basis set 4-31G (see e.g. Frish et al. 1984) to expand the molecular orbitals. This method, extensively used in the literature, has been shown to be particularly suitable for the vibrational analysis of PAHs (Langhoff 1996; Bauschlicher & Langhoff 1997; Hudgins et al. 2001; Bauschlicher Jr. 2002). Moreover, when an excited state of interest and the ground state are of different symmetry, it is possible to study even the former using the B3LYP method, which yields reliable results provided that the excited state be well described by a single determinant electronic wavefunction (Halasinski et al. 2000).

We focused on the second electronic transition ($D_0 \rightarrow D_2$) of $C_{32}H_{14}^{+}$, the first one being forbidden. In D_{2h} point group notation this transition is from state B_{2g} to A_u. According to previous results on smaller D_{2h} molecules (Negri & Zgierski 1994; Hirata et al. 1999), the D_2 excited state is well represented by the electronic promotion H-1→ S, where S is the singly occupied Molecular Orbital (MO) in the ground state configuration, H is the highest completely occupied MO and H-1 is the one just below it. The excitation energy, as evaluated from the total energy difference $E_N^{TOT} - E_N^{TOT}(\star)$ between the ground state energy of the molecule and that of the excited one, is 1.34 eV, close to the experimental value in Ne matrix of 1.27 eV (Ehrenfreund et al. 1995; Ruiterkamp et al. 2002).

The ground state optimised geometry of $C_{32}H_{14}^{+}$ at the B3LYP/4-31G level of theory is displayed in Fig. 5.

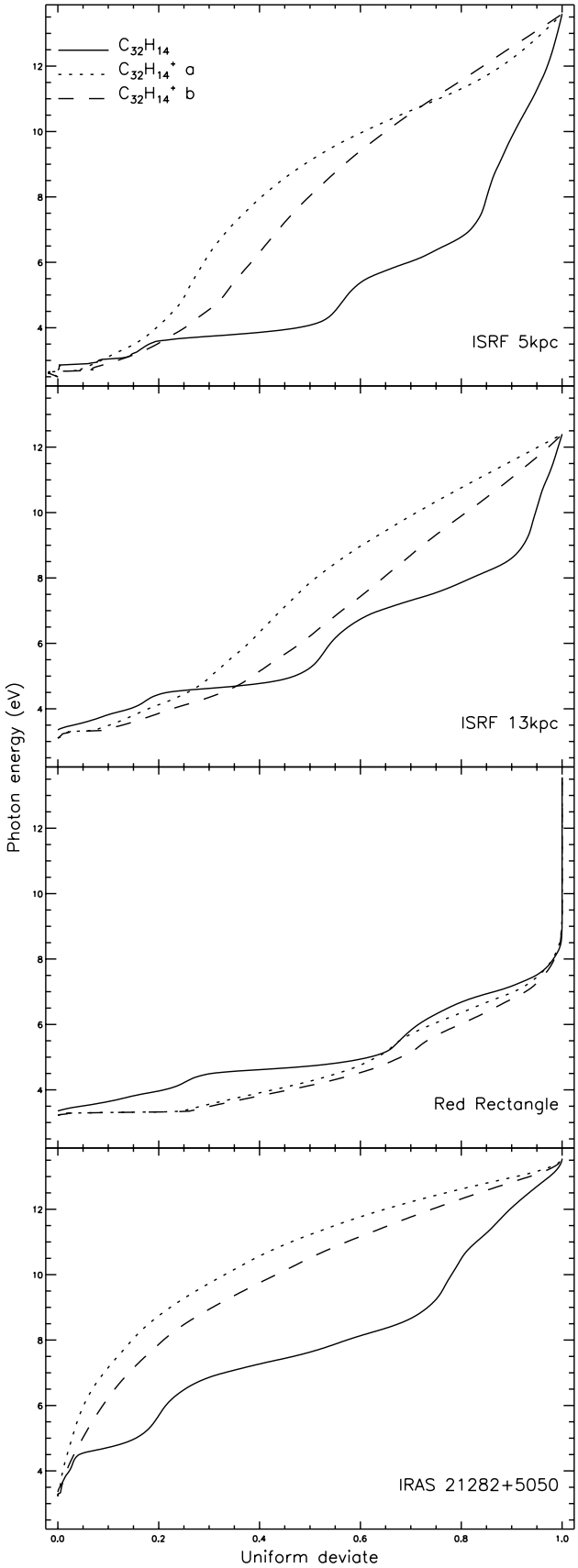

Fig. 4. Function transforming uniform deviates in the range $(0, 1)$ in energy of photons absorbed by the ovalene neutral and cation according to the probability distribution in Fig. 3.

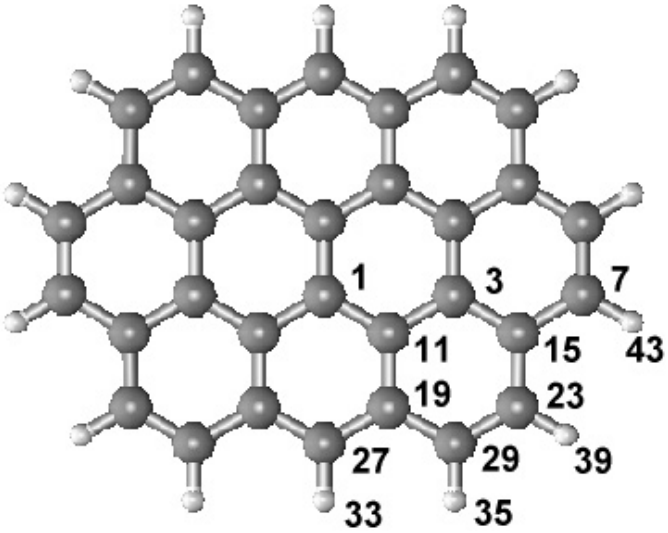

Fig. 5. Ground state geometry of $C_{32}H_{14}$ showing the 9 inequivalent C atoms (labelled by 1, 3, 7, 11, 15, 19, 23, 27 and 29) and the 4 inequivalent H atoms (labelled by 33, 35, 39 and 43); the molecule lies in the *xy*-plane, the *y*-axis being the longer one.

Table 3. Ab initio principal momenta of inertia (in a.m.u. Å^2) for the D_0 and D_2 electronic states of $C_{32}H_{14}^+$ as obtained at B3LYP/4-31G level of theory; last column shows the effect of geometry distortion following the excitation of the molecule.

Property	$D_0(B_{2g})$	$D_2(A_u)$	Delta
I*x*	3442	3457	+15
I*y*	2112	2111	−1
I*z*	5554	5568	+14

The momenta of inertia of the optimised geometry of both the ground (D_0) and excited (D_2) states are shown in Table 3. The study of the difference in the geometries of the two states involved in the transition is essential, since it determines the asymmetry (red shading, in this case) of the rotational envelope of the vertical absorption band.

The computation of harmonic vibrational frequencies was performed at the optimised geometry using the usual projection operator technique (Wilson Jr. et al. 1955). For each of the 132 vibrational normal modes we obtained frequency, symmetry and, for the 56 IR-active ones, the Einstein coefficient of the (0−1) pure vibrational transition, both for the neutral and ovalene cation. The frequencies of all the modes are used within the Monte-Carlo model to compute the density of vibrational states as a function of energy, while the intensities and symmetries are used to simulate the IR cascades. Our results are in good agreement with the values published by Langhoff (1996). As a computationally free by-product we also obtained the zero-point harmonic vibrational energies, for the most likely single isotopic substitutions, i.e. $^{13}C \rightarrow {}^{12}C$ and $D \rightarrow H$. This sums up to 9 inequivalent C atom and 4 inequivalent H atom substitutions (see Fig. 5). The complete list of frequencies and

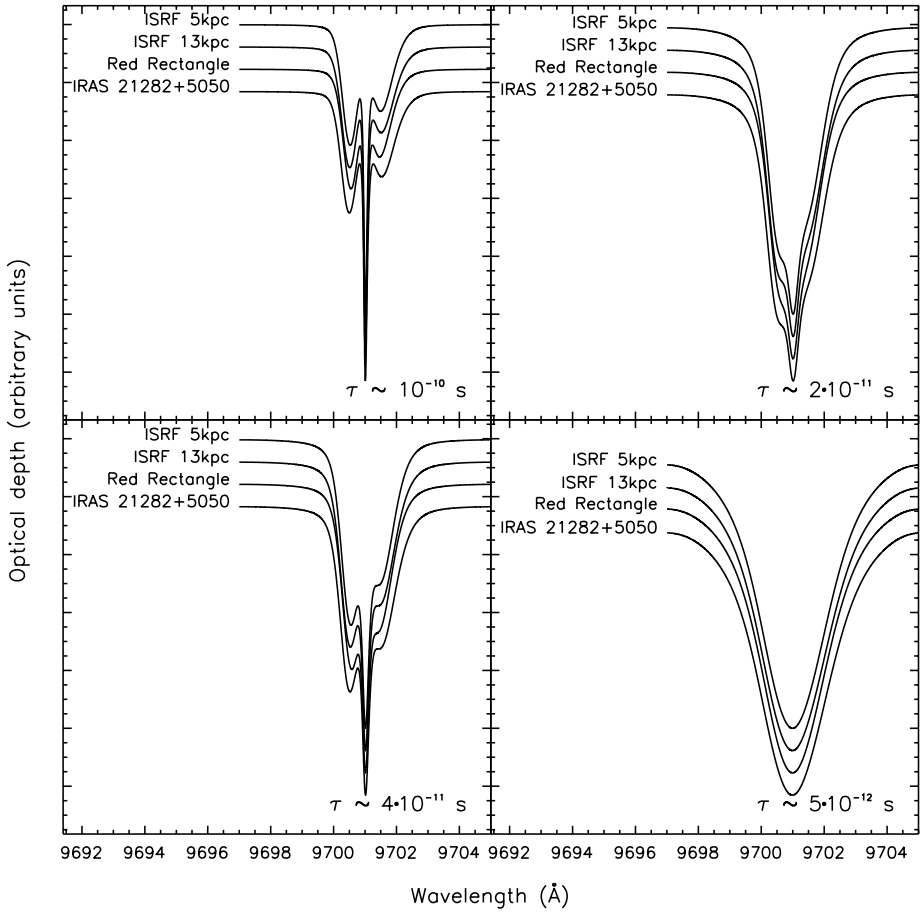

Fig. 6. Comparison of the expected rotational profiles of the $D_0 \rightarrow D_2$ band of $C_{32}H_{14}^+$, assuming it to be in rotational statistical equilibrium in that state, for four very different incident radiation fields and decay times of the excited state ranging from 10^{-10} to 5×10^{-12} s.

corresponding intensities, for all the inequivalent isotopic substitutions can be found in Malloci (2003).

4. Results

Using a compendium of calculated and experimental data about $C_{32}H_{14}$ and $C_{32}H_{14}^+$, our Monte-Carlo model simulated their UV/Vis pumping and the consequent IR cooling cascades for a multidimensional grid of variable parameters. In particular, for the ISRF of Mathis et al. (1983) corresponding to a galactocentric distance of 5 kpc we considered four different ionisation equilibria. In the two extreme cases the molecule is allowed to reach its equilibrium statistical population of rotational levels respectively as a cation and as a neutral, while in the two intermediate ones it was followed along a series of subsequent ionisations and recombinations. We also ran simulations for an ISRF at 13 kpc and for the radiation fields of the Red Rectangle reflection nebula and of the IRAS 21282+5050 planetary nebula, assuming in both cases the molecule to be located about 1″ away from the central source. For these radiation fields we only considered the two extreme ionisation equilibria above. This was actually done just for the sake of completeness, since the molecule under study can be expected to be almost always neutral in the Red Rectangle and almost always ionised in IRAS 21282+5050. Furthermore, we ran the model independently using the two different estimates of the $\sigma_{\rm abs}(E)$ of $C_{32}H_{14}^+$ in the VUV provided by Robinson et al. (1997), in order to explicitly evaluate the impact of this particular source of indetermination.

Figure 6 shows the expected rotational profile of the $D_0 \rightarrow D_2$ band of $C_{32}H_{14}^+$, as it would be observed in four different radiation fields and for four different lifetimes of the excited state ranging from 10^{-10} to 5×10^{-12} s. We assumed the band origin to lie at a wavelength of 9701 Å (Ehrenfreund & Foing 1996). The precise position of this band is actually still uncertain (Ruiterkamp et al. 2002), but this is irrelevant for the present work, which concerns the spectral profile. The lifetime of the excited electronic state for PAH-like molecules can be as short as 10^{-12} s, against the 10^{-8} s typical of an electronic transition involving the emission of radiation (Birks 1970). Indeed, according to recent results by Bréchignac et al. (2001), the measured lorentzian broadening in electronic transitions of the naphtalene cation hints at excited state lifetimes even slightly shorter than 10^{-12} s. The rotational fine structure of the band is progressively smoothed out for decreasing lifetimes, leaving just a barely detectable asymmetry in the most extreme case we considered here. The rotational profile of the modelled electronic absorption band expected for the different ionization equilibria considered are presented in Fig. 7 in four different radiation fields. The curves in each box correspond

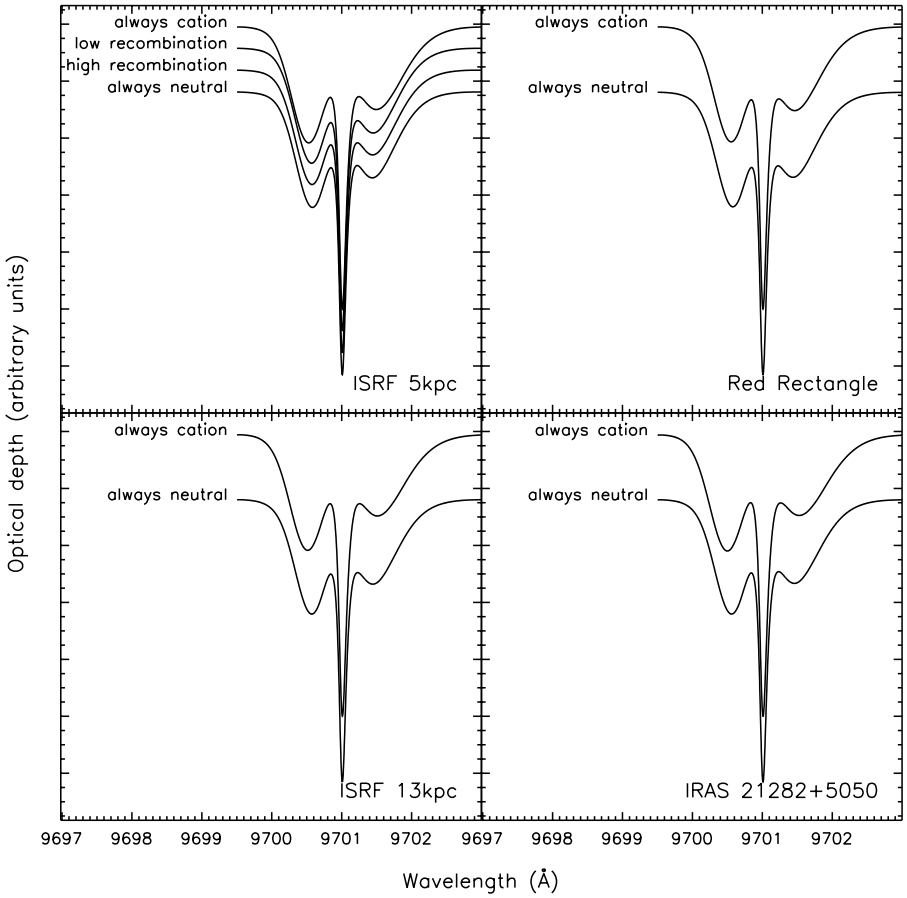

Fig. 7. Comparison of the expected rotational profiles of the $D_0 \rightarrow D_2$ band of $C_{32}H_{14}^+$, assuming it to be respectively in rotational statistical equilibrium as a cation, as its parent neutral molecule, or simulating a sequence of ionisations and recombinations. The four boxes correspond to four very different incident radiation fields (see text).

to $C_{32}H_{14}^+$ being in rotational statistical equilibrium respectively as a cation, as its parent neutral molecule, and assuming two different networks neutral-cation. More specifically, from bottom to top the curves correspond to decreasing electronic recombination rates, namely 1.3×10^{-7} (Eq. (1)), 1.7×10^{-8} (Eq. (2)), 5.2×10^{-9} (Eq. (3)) and $<10^{-10}$ s^{-1} (limiting case). These recombination rates govern the fraction of time which the molecule spends in its neutral state versus the time which it spends as a cation, ranging from being almost always neutral for recombination rates $\geq 1.3 \times 10^{-7}$ s^{-1} to being almost always ionised for rates $\leq 10^{-10}$ s^{-1}.

The extreme cases were modelled simply considering respectively the statistical equilibrium of the isolated neutral molecule and of the isolated cation; the two intermediate cases were obtained following the populations of rotational levels through a sequence of ionizations (according to Eq. (4) with the corresponding $R_{\rm ion}$ and $R_{\rm abs}^{\rm N}$) and recombinations (according to Eq. (5) with the corresponding $R_{\rm rec}$). No detectable differences in the profiles thus obtained can be seen. Finally, Fig. 8 shows that the difference between the results obtained considering Robinson et al. (1997)'s "a" and "b" estimates for the VUV absorption cross section of the cation is completely negligible in all of the four different radiation fields examined here.

One more source of fine structure expected to be present in vibronic absorption spectra of molecules like $C_{32}H_{14}^+$ is the difference in zero-point vibrational energies due to isotopic substitutions (Webster 1996; Walker et al. 2000). We considered here only the most likely single atom substitutions, namely $^{12}C \rightarrow ^{13}C$ and $D \rightarrow H$, for which we obtained the band shifts listed in Table 4 for the (0−0) vertical electronic transition.

Finally, the fraction of the total emitted energy and the fraction of the total emitted number of photons in each infrared band output from our model, are shown in Tables 5 and 6 for both $C_{32}H_{14}$ and $C_{32}H_{14}^+$ assumed in the ISRF-5 kpc radiation field of Mathis et al. (1983). To make these tables more readable, bands very close in energy were grouped together.

5. Discussion

Despite the wide range of variability of the parameters considered in this work, we obtained only minimal differences among the resulting rotational profiles obtained. The only barely detectable difference (on noiseless synthetic spectra!) corresponds to the hardest radiation field, the one of the planetary nebula. However, DIBs have never been observed so far in such an environment, we included its simulation only as an extreme situation of the excitation conditions examined.

Since in our model the rotation of the molecule is by and large determined by the balance of infrared photons emitted in

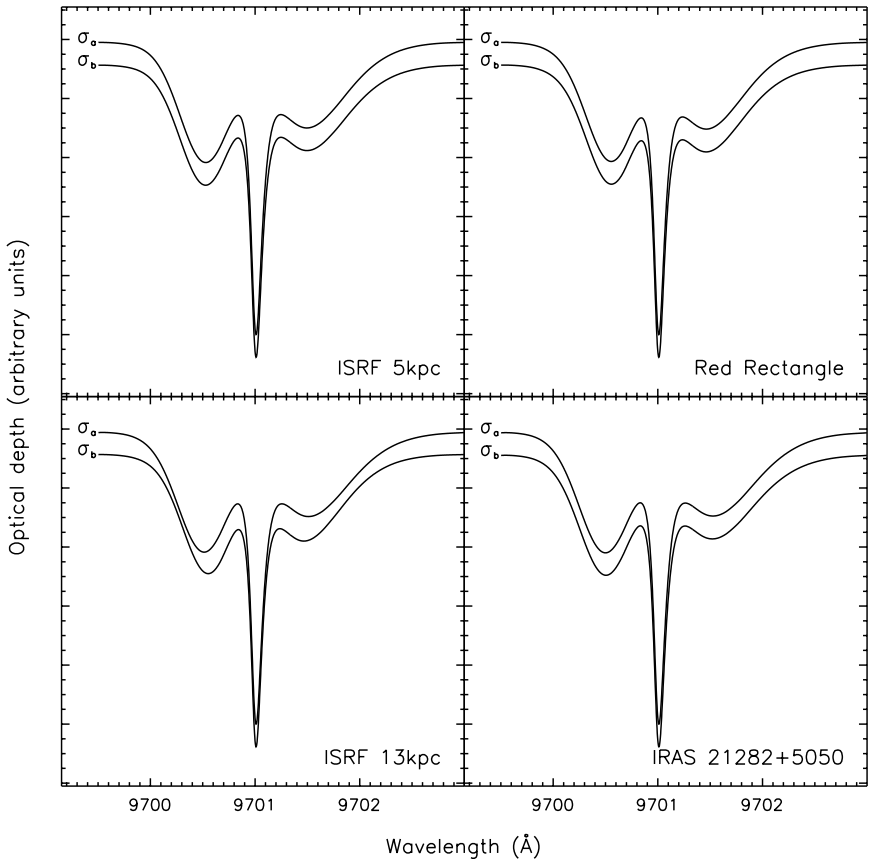

Fig. 8. Comparison of the expected rotational profiles of the $D_0 \rightarrow D_2$ band of $C_{32}H_{14}^+$, assuming it to be in rotational statistical equilibrium using respectively approximation (a) and approximation (b) given by Robinson et al. (1997) for its VUV absorption cross section. The four boxes correspond to four very different incident radiation fields.

Table 4. Wavelength shift (in Å) of the (0−0) vertical electronic transition due to the most likely isotopic substitutions $^{12}C \rightarrow ^{13}C$ and $D \rightarrow H$ in the 13 inequivalent atom positions labelled in Fig. 5.

Isotopic substitution	shift (Å)
$^{13}C \rightarrow ^{12}C$ in 1	3.7×10^{-3}
$^{13}C \rightarrow ^{12}C$ in 3	5.2×10^{-4}
$^{13}C \rightarrow ^{12}C$ in 7	4.9×10^{-4}
$^{13}C \rightarrow ^{12}C$ in 11	5.8×10^{-4}
$^{13}C \rightarrow ^{12}C$ in 15	5.6×10^{-3}
$^{13}C \rightarrow ^{12}C$ in 19	6.9×10^{-3}
$^{13}C \rightarrow ^{12}C$ in 23	4.2×10^{-3}
$^{13}C \rightarrow ^{12}C$ in 27	8.7×10^{-3}
$^{13}C \rightarrow ^{12}C$ in 29	1.8×10^{-3}
D → H in 33	1.4×10^{-2}
D → H in 35	1.6×10^{-2}
D → H in 39	1.6×10^{-2}
D → H in 43	1.7×10^{-2}

the cooling cascades (see e.g. Rouan et al. 1992; Mulas 1998), the reasons for such a remarkable invariance should be sought in Tables 5 and 6, in particular in the columns which list the fraction of photons emitted in different groups of bands. In a qualitative way, the higher the energy of the emitted IR photons, the faster the molecule will tend to rotate. It can be easily seen that while the *energy* fraction emitted in the highest energy bands changes considerably for different radiation fields, the *photon* fractions (in number) are much less affected. In particular, for the neutral molecule a harder radiation fields translates mainly in stronger emission near 3 μm, which nonetheless are a negligible fraction of the emitted photons *in number*. Similarly for the cation, relatively considerable changes in the energy fraction emitted in high energy vibrational modes translate in very much smaller changes when the numbers of photons are considered.

It is more intriguing to understand why the cation and the neutral molecule reach almost undistinguishable rotational statistical equilibria: in this case, the main difference (in photon number fraction) is that the reduced emission in the cation in the C-H out of plane bending mode around 11 μm (~13% of the photons compared to ~26% in the neutral) is balanced by an increase *both* in the photons emitted in the two lowest energy out of plane skeletal bending modes at about ~85 and ~150 μm respectively (~49% against ~40%) *and* the relatively higher energy in plane C-C stretches and C-H bendings in the 6−8 μm range (17% against 6%). The net effects coincidentally almost cancel. These changes between neutral and cation are not at all peculiar of ovalene, but instead are quite general among

Table 5. IR active bands of $C_{32}H_{14}$, grouped in small energy ranges, in the four different radiation fields considered, along with the respective fractions of total emitted energy and total emitted photons. Bands with a photon number fraction below 0.1% were omitted.

Wavelength range (μm)	Number of modes	ISRF 5 kpc		ISRF 13 kpc		Red Rectangle		IRAS 21282+5050	
		Energy fraction %	Photon fraction %	Energy fraction %	Photon fraction %	Energy fraction %	Photon fraction %	Energy fraction %	Photon fraction %
3.13–3.15	7	3.4	0.5	3.4	0.5	2.3	0.3	5.1	0.8
5.93–6.22	4	3.0	0.9	3.3	1.0	2.7	0.8	3.6	1.1
6.30–6.58	3	1.3	0.4	1.3	0.4	1.2	0.4	1.5	0.5
6.67–6.99	6	1.6	0.5	1.6	0.5	1.5	0.5	1.8	0.7
7.27–7.35	2	4.0	1.4	4.1	1.4	3.9	1.3	4.5	1.7
7.50–7.89	4	2.6	1.0	2.5	1.0	2.6	0.9	2.8	1.1
8.12–8.26	3	4.9	1.9	5.1	2.0	4.9	1.8	5.2	2.2
9.85–9.93	2	0.4	0.2	0.4	0.2	0.4	0.2	0.4	0.2
10.52–10.71	2	26.9	13.8	27.3	14.3	27.3	13.6	27.2	15.4
11.37	1	16.2	8.8	16.5	9.2	16.5	8.8	16.3	9.8
12.32–12.40	3	2.8	1.6	2.9	1.7	2.9	1.6	2.8	1.8
12.58	1	0.6	0.4	0.7	0.4	0.6	0.4	0.6	0.4
13.60	1	0.6	0.4	0.6	0.4	0.6	0.4	0.6	0.4
14.40–14.62	2	0.2	0.1	0.2	0.1	0.2	0.1	0.2	0.1
15.23	1	6.4	4.7	6.3	4.7	6.5	4.7	6.1	4.9
16.72	1	1.2	1.0	1.2	1.0	1.3	1.0	1.1	1.0
17.65–17.72	2	3.7	3.2	3.5	3.1	3.8	3.1	3.3	3.1
19.58	1	0.2	0.2	0.2	0.2	0.2	0.2	0.2	0.2
22.58	1	1.0	1.1	1.0	1.1	1.0	1.1	0.9	1.0
24.53	1	2.7	3.2	2.6	3.1	2.7	3.1	2.4	3.1
28.19	1	3.2	4.4	3.1	4.4	3.4	4.5	2.7	4.1
35.16	1	4.0	6.8	3.8	6.6	4.1	6.8	3.4	6.3
89.42	1	6.4	27.3	6.1	26.8	6.6	27.4	5.4	25.2
153.51	1	2.1	15.2	1.9	14.6	2.2	15.6	1.7	13.6

compact PAHs, hence this effect on molecular rotation can be safely expected to hold for the whole class.

Beyond the very weak, if any, dependence on the assumed environmental conditions, the DIB profiles predicted by our Monte-Carlo model seem to be by and large independent of the most poorly known molecular parameters, i.e. the ionization fraction and the VUV absorption spectrum of the particular species under study. This is, on the one hand, a happy coincidence, which grants to our model a stronger predictive power than could be a priori anticipated; on the other hand, it makes PAH electronic absorption band profiles poor diagnostic tools to estimate those same poorly known parameters. In fact, the results of our code depend only on some basic parameters of the modelled molecule, which are either currently available from experiments or can be easily obtained with quantum-chemical calculations, such as the whole vibrational spectrum or the absorption spectrum in the UV/Vis/NIR spectral range. As a consequence, rotational profile invariace can be expected to be not peculiar of the specific molecular species considered, but instead to be valid at least for this whole class of molecules, i.e. saturated PAHs, which share very similar properties and similar differences between the neutral molecule and the respective parent cation. This provides a sound *quantitative* foundation to the hypothesis of PAHs as DIB carriers, since profile stability in spite of changing physical environment is one of their most prominent observed properties.

Concerning isotopic substitutions, our results show this to be utterly irrelevant for the specific (0–0) vibronic band modelled here, since band shifts are orders of magnitude smaller than the width of the rotational envelope, and thus would not be detectable under any conditions (cf. Table 4).

6. Conclusions and future work

Using ab initio calculations, available experimental data and our Monte-Carlo model, we modelled the expected spectral profile of a vibronic transition of $C_{32}H_{14}^{+}$. This spectral profile resulted to be remarkably insensitive to ambient conditions, yielding one more quantitative confirmation that PAH cations fulfil one of the most stringent requirements for good candidate

Table 6. IR active bands of $C_{32}H_{14}^{+}$, grouped in small energy ranges, in the four different radiation fields considered, along with the respective fractions of total emitted energy and total emitted photons. Bands with a photon number fraction below 0.1% were omitted.

Wavelength range (μm)	Number of modes	ISRF 5 kpc		ISRF 13 kpc		Red Rectangle		IRAS 21282+5050	
		Energy fraction %	Photon fraction %	Energy fraction %	Photon fraction %	Energy fraction %	Photon fraction %	Energy fraction %	Photon fraction %
3.10−3.13	7	1.5	0.3	1.3	0.2	0.7	0.1	1.9	0.3
6.03−6.24	4	11.1	3.7	10.9	3.5	8.7	2.4	12.2	4.3
6.35−6.54	3	1.1	0.4	1.0	0.3	0.9	0.3	1.0	0.4
6.75−6.98	6	6.1	2.3	5.8	2.1	5.1	1.6	6.2	2.5
7.19−7.39	2	14.7	5.8	14.7	5.6	12.7	4.2	15.2	6.3
7.52−7.84	3	5.4	2.3	5.3	2.2	5.1	1.8	5.5	2.4
7.92−8.30	4	7.5	3.3	7.0	3.0	6.7	2.5	7.4	3.5
8.97−8.98	2	0.2	0.1	0.3	0.1	0.2	0.1	0.3	0.1
9.66−9.87	2	0.1	0.1	0.2	0.1	0.2	0.1	0.2	0.1
10.39−10.51	2	12.9	7.4	13.0	7.2	12.8	6.2	12.7	7.7
11.07	1	11.0	6.7	11.4	6.7	11.9	6.1	11.0	7.1
11.96−12.42	3	4.7	3.1	4.8	3.1	5.1	2.9	4.7	3.3
12.63	1	0.1	0.1	0.1	0.1	0.1	0.1	0.1	0.1
14.38−15.14	3	5.3	4.2	5.4	4.2	6.1	4.1	5.0	4.2
16.90−17.52	2	0.2	0.2	0.2	0.2	0.3	0.2	0.2	0.2
17.70	1	3.1	3.1	3.2	3.0	3.6	3.0	2.9	3.0
19.33	1	0.3	0.3	0.3	0.3	0.4	0.3	0.3	0.3
24.84	1	2.8	3.7	2.9	3.8	3.5	3.9	2.6	3.6
27.60	1	1.7	2.5	1.7	2.5	2.1	2.7	1.5	2.4
33.73	1	0.1	0.1	0.1	0.1	0.1	0.2	0.0	0.1
44.30	1	0.3	0.8	0.3	0.8	0.4	0.9	0.3	0.7
83.45	1	7.7	34.8	8.1	35.6	10.3	39.1	6.9	33.3
150.81	1	1.7	13.9	1.8	14.3	2.3	16.2	1.5	13.1

carriers of the Diffuse Interstellar Bands. Specifically, these results will be useful for a definitive assessment on the presence of the $C_{32}H_{14}^{+}$ molecule in interstellar space, since they provide one more constraint to be matched for an unambiguous identification.

We also showed this approach to be generally feasible, at least, for the whole class of PAH molecules and cations, and demonstrated its potential in providing an independent identification criterion for potential DIB carriers. Our long term aim will be to systematically apply the above analysis to a large sample of astrophysically relevant molecules. With more computational tools providing Time Dependent DFT becoming more reliable and commonly available (see e.g. Weisman et al. 2003), we expect to be able to obtain ab initio electronic excitation energies and absorption spectra of PAHs, at least up to excitation energies of a few eVs (Hirata et al. 1999; Weisman et al. 2001, 2003). This will provide a completely self-contained computational tool which will be a valuable guide for targeted experiments and observations.

Acknowledgements. The authors thank the referee who helped improve the paper with useful comments. G. Malloci gratefully acknowledges the financial support by INAF – Osservatorio Astronomico di Cagliari. The authors are thankful to Prof. G. Cappellini and Dr. G. Satta for their help with ab initio methodologies. We acknowledge the High Performance Computational Chemistry Group for using their code: "NWChem, A Computational Chemistry Package for Parallel Computers, version 4.0.1" (2001), Pacific Northwest National Laboratory, Richland, Washington, USA.

References

Abouelaziz, H., Gomet, J. C., Pasquerault, D., & Rowe, B. R. 1993, J. Chem. Phys., 99, 237
Allain, T., Leach, S., & Sedlmayr, E. 1996a, A&A, 305, 602
Allain, T., Leach, S., & Sedlmayr, E. 1996b, A&A, 305, 616
Allamandola, L. J., Tielens, G. G. M., & Barker, J. R. 1989, ApJS, 71, 733
Bakes, E. L. O., Tielens, A. G. G. M., & Bauschlicher, C. W. 2001a, ApJ, 556, 501
Bakes, E. L. O., Tielens, A. G. G. M., Bauschlicher, C. W., Hudgins, D. M., & Allamandola, L. J. 2001b, ApJ, 560, 261
Bally, T. 2002, private communication
Bauschlicher, C. W., & Langhoff, S. R. 1997, Spectrochim. Acta Part A, 53, 1225

Bauschlicher Jr., C. W. 2002, ApJ, 564, 782
Becke, A. D. 1993, J. Chem. Phys., 98, 5648
Bernstein, M. P., Sandford, S. A., Allamandola, L. J., et al. 1999, Science, 283, 1135
Birks, J. B. 1970, Photophysics of Aromatic Molecules (London: Wiley-Interscience)
Bréchignac, P., Pino, T., & Boudin, N. 2001, Spectrochim. Acta, 57, 745
Cardelli, J. A., Meyer, D. M., Jura, M., & Savage, B. D. 1996, ApJ, 467, 334
Cernicharo, J., Heras, A. M., Tielens, A. G. G. M., et al. 2001, ApJ, 546, L123
Cohen, M. E. A. 1975, ApJ, 196, 179
Cossart-Magos, C., & Leach, S. 1990, A&A, 233, 559
Crawford, M. K., Tielens, A. G. G. M., & Allamandola, L. J. 1985, ApJ, 293, L45
Dartois, E., & D’Hendecourt, L. 1997, A&A, 323, 534
Ehrenfreund, P., Cami, J., Jiménez-Vicente, J., et al. 2002, ApJ, 576, L117
Ehrenfreund, P., & Charnley, S. B. 2000, ARA&A, 38, 427
Ehrenfreund, P., D’Hendencourt, L., Verstraete, L., et al. 1992, A&A, 259, 257
Ehrenfreund, P., & Foing, B. H. 1996, A&A, 307, L25
Ehrenfreund, P., Foing, B. H., D’Hendecourt, L., Jenniskens, P., & Déesert, F. X. 1995, A&A, 299, 213
Eilfeld, P., & Schmidt, W. 1981, J. Elect. Spectrosc. Rel. Phenom., 24, 101
Foing, B. H., & Ehrenfreund, P. 1994, Nature, 369, 296
Frish, M. J., Pople, J. A., & Binkley, J. S. 1984, J. Chem. Phys., 80, 3265
Galazutdinov, G., Stachowska, W., Musaev, F., et al. 2002, A&A, 396, 987
Galazutdinov, G. A., Musaev, F. A., Krełowski, J., & Walker, G. A. H. 2000, PASP, 112, 648
GNU Scientific Library. 2001, GSL, available on the web from `http://www.gnu.org/software/gsl/gsl.html`
Gondhalekar, P., Philips, A., & Wilson, R. 1980, A&A, 85, 272
Gudipati, M. 2002, private communication
Halasinski, T. M., Hudgins, D. M., Salama, F., & Allamandola, L. J. 2000, J. Phys. Chem. A, 104, 7484
Harrison, R. J., Nichols, J. A., Straatsma, T. P., et al. 2001, NWChem, A Computational Chemistry Package for Parallel Computers, Version 4.0.1
Herbig, G. H. 1995, ARA&A, 33, 19
Herzberg, G. 1991a, Electronic Spectra and Electronic Structure of Polyatomic Molecules, Vol. 3 of Molecular Spectra and Molecular Structure (Krieger Drive, Malabar, Florida: Krieger Publishing Company)
Herzberg, G. 1991b, Infrared and Raman Spectra of Polyatomic Molecules, Vol. 2 of Molecular Spectra and Molecular Structure (Krieger Drive, Malabar, Florida: Krieger Publishing Company)
Hirata, S., Lee, T., & Head-Gordon, M. 1999, J. Chem. Phys., 111, 8904
Hudgins, D. M., Bauschlicher, C. W., & Allamandola, L. J. 2001, Spectrochim. Acta Part A, 57, 907
Jenniskens, P., & Desert, F.-X. 1994, A&AS, 106, 39
Jenniskens, P., Porceddu, I., Benvenuti, P., & Desert, F.-X. 1996, A&A, 313, 649
Joblin, C. 1992, Ph.D. Thesis, Université Paris 7
Joblin, C., Léger, A., & Martin, P. 1992, ApJ, 393, L79
Kerr, T. H., Hibbins, R. E., Fossey, S. J., Miles, J. R., & Sarre, P. J. 1998, ApJ, 495, 941
Kerr, T. H., Hibbins, R. E., Miles, J. R., et al. 1996, MNRAS, 283, L105
Kin-Wing, C., Roellig, T. L., Onaka, T., et al. 2001, ApJ, 546, 273
Krelowski, J., & Schmidt, M. 1997, ApJ, 477, 209
Kurucz, R. 1992, in The Stellar Populations of Galaxies, ed. B. Barbuy, & A. Renzini, IAU Symposium 149 (Dordrecht: Kluwer Academic Publishers), 225
Langhoff, S. R. 1996, J. Phys. Chem, 100, 2819
Le Page, V., Snow, T. P., & Bierbaum, V. M. 2001, ApJS, 132, 233
Leach, S. 1995, Planet. Space Sci., 43, 1153
Léger, A., & D’Hendecourt, L. 1985, A&A, 146, 81
Léger, A., D’Hendecourt, L., & Defourneau, D. 1989, A&A, 216, 148
Malloci, G. 2003, Ph.D. Thesis, Università degli Studi di Cagliari
Mathis, J. S., Mezger, P. G., & Panagia, N. 1983, A&A, 128, 212
Men’shchikov, A. B., Balega, Y. Y., Osterbart, G., & Weigelt, G. 1998, New Astron., 3, 601
Motylewski, T., Linnartz, H., Vaizert, O., et al. 2000, ApJ, 531, 312
Mulas, G. 1998, A&A, 338, 243
Negri, F., & Zgierski, M. Z. 1994, J. Phys. Chem., 100, 2819
Omont, A. 1986, A&A, 164, 159
Pech, C., Joblin, C., & Boissel, P. 2002, A&A, 388, 639
Robinson, M. S., Beegle, L. W., & Wdowiak, T. J. 1997, ApJ, 474, 474
Rouan, D., Léger, A., Omont, A., & Giard, M. 1992, A&A, 253, 498
Ruiterkamp, R., Halasinski, T., Salama, F., et al. 2002, A&A, 390, 1153
Salama, F. 1999, in Solid Interstellar Matter: The ISO Revolution, Les Houches Workshop, February 2−6, 1998, ed. L. d’Hendecourt, C. Joblin, & A. Jones (EDP Sciences and Springer-Verlag), 65
Salama, F. 2002, private communication
Salama, F., Bakes, E. L. O., Allamandola, L. J., & Tielens, A. G. G. M. 1996, ApJ, 458, 621
Salama, F., Galazutdinov, G. A., Krełowski, J., Allamandola, L. J., & Musaev, F. A. 1999, ApJ, 526, 265
Sarre, P. J., Miles, J. R., Kerr, T. H., et al. 1995, MNRAS, 277, L41
Sloan, G. C., Grasdalen, G. L., & LeVan, P. D. 1993, ApJ, 416, 409
Snow, T. P., & Witt, A. N. 1995, Science, 270, 1455
Tuairisg, S. Ó., Cami, J., Foing, B. H., Sonnentrucker, P., & Ehrenfreund, P. 2000, A&AS, 142, 225
Tulej, M., Kirkwood, D. A., Pachkov, M., & Maier, J. P. 1998, ApJ, 506, L69
van der Zwet, G. P., & Allamandola, L. 1985, A&A, 146, 76
Verstraete, L., Léger, A., D’Hendecourt, L., Dutuit, O., & Défourneau, D. 1990, A&A, 237, 436
Vuong, M. H., & Foing, B. H. 2000, A&A, 363, L5
Walker, G. A. H., Bohlender, D. A., & Krełowski, J. 2000, ApJ, 530, 362
Walker, G. A. H., Webster, A. S., Bohlender, D. A., & Krełowski, J. 2001, ApJ, 561, 272
Webster, A. 1996, MNRAS, 282, 1372
Weisman, J. L., Lee, T. J., & Head-Gordon, M. 2001, Spectrochim. Acta Part A, 57, 931
Weisman, J. L., Lee, T. J., Salama, F., & Head-Gordon, M. 2003, ApJ, 587, 256
Weselak, T., Schmidt, M., & Krełowski, J. 2000, A&AS, 142, 239
Wilson Jr., B., Decius, J. C., & Cross, P. C. 1955, Molecular Vibrations - The theory of Infrared and Raman Vibrational Spectra (New York: McGraw-Hill)
Woods, P. M., Millar, T. J., Zijlstra, A. A., & Herbst, E. 2002, ApJ, 574, L167